

*Università degli Studi di Padova*

*Padua Research Archive - Institutional Repository*

The bone marrow functionally contributes to liver fibrosis

*Original Citation:*

*Availability:*

This version is available at: 11577/1564888 since:

*Publisher:*

*Published version:*

DOI: 10.1053/j.gastro.2006.01.036

*Terms of use:*

Open Access

This article is made available under terms and conditions applicable to Open Access Guidelines, as described at <http://www.unipd.it/download/file/fid/55401> (Italian only)

(Article begins on next page)

# The Bone Marrow Functionally Contributes to Liver Fibrosis

FRANCESCO P. RUSSO,\* MALCOLM R. ALISON,† BRIAN W. BIGGER,§ EUNICE AMOFAH,\* AIKATERINI FLOROU,\* FARHANA AMIN,\* GEORGE BOU-GHARIOS,¶ ROSEMARY JEFFERY,|| JOHN P. IREDALE,\*\* and STUART J. FORBES\*

\*Department of Medicine, Imperial College, London; †Department of Diabetes and Medicine, Queen Mary University of London, London; §Stem Cell Research Laboratory, National Blood Service, John Radcliffe Hospital, Oxford; ¶Renal Laboratory, Hammersmith Hospital, Imperial College, London; ||Histopathology Unit, Cancer Research UK, London; and \*\*Tissue Fibrosis and Repair Group, MRc University of Edinburgh Centre for Inflammation Research, United Kingdom

**Background & Aims:** Bone marrow (BM) cells may transdifferentiate into or fuse with organ parenchymal cells. BM therapy shows promise in murine models of cirrhosis, and clinical trials of bone marrow stem cell therapy for organ healing are underway. However, the BM may contribute to scar-forming myofibroblasts in various organs including the liver. We have studied this axis of regeneration and scarring in murine models of cirrhosis, including an assessment of the temporal and functional contribution of the BM-derived myofibroblasts. **Methods:** Female mice were lethally irradiated and received male BM transplants. Carbon tetrachloride or thioacetamide was used to induce cirrhosis. BM-derived cells were tracked through in situ hybridization for the Y chromosome. BM transplants from 2 strains of transgenic mice were used to detect intrahepatic collagen production. **Results:** In the cirrhotic liver, the contribution of BM to parenchymal regeneration was minor (0.6%); by contrast, the BM contributed significantly to hepatic stellate cell (68%) and myofibroblast (70%) populations. These BM-derived cells were found to be active for collagen type 1 transcription in 2 independent assays and could influence the fibrotic response to organ injury. These BM-derived myofibroblasts did not occur through cell fusion between BM-derived cells and indigenous hepatic cells but, instead, originated largely from the BM's mesenchymal stem cells. **Conclusions:** The BM contributes functionally and significantly to liver fibrosis and is a potential therapeutic target in liver fibrosis. Clinical trials of BM cell therapy for liver regeneration should be vigilant for the possibility of enhanced organ fibrosis.

There have been claims that bone marrow (BM) stem cells may differentiate into cells within organs previously thought to regenerate only from local tissue stem cells.<sup>1-4</sup> However, this so-called “plasticity” may be limited in extent or result from the fusion of BM-derived cells and recipient somatic cells.<sup>5,6</sup> In the liver, BM transplant has been shown to cure the fumarylacetoacetate hydrolase-deficient (Fah<sup>-/-</sup>) mouse, a murine model of hereditary

tyrosinemia.<sup>7</sup> Initially thought to occur through stem cell plasticity,<sup>8</sup> this cure was later shown to occur through cell fusion of donor BM-derived macrophages with the recipient hepatocytes. Although the therapeutic repopulation of liver parenchyma by BM-derived hepatocytes in a mouse model of cirrhosis is reported,<sup>9</sup> this has not been found in similar liver damage models.<sup>10-12</sup> There has been recognition that many nonparenchymal cell populations are at least in part of BM origin, such as the hepatic endothelium<sup>13</sup> and scar-associated macrophages.<sup>14</sup> Hepatic stellate cells occupy the space of Disse; following injury, they become activated into a myofibroblast phenotype and produce collagen.<sup>15-17</sup> Stellate cells have been thought to be of neural crest origin; however, recent data indicate that their histogenesis may be more complex. Circulating BM-derived myofibroblasts are prominent in a number of organs.<sup>18-20</sup> Hepatic stellate cells of BM origin have been identified in mouse models,<sup>21</sup> and a proportion of hepatic myofibroblasts are of BM origin in human liver fibrosis.<sup>22</sup> Fractionated BM injections have been used in a murine model to ameliorate CCl<sub>4</sub>-induced liver fibrosis.<sup>23</sup> Studies such as this have encouraged the investigation of BM therapy in chronic organ injury and regeneration.<sup>24</sup> Knowledge of the specific BM-derived cells mediating both the profibrotic and therapeutic response in injured organs is critical for the rational planning of clinical trials of BM stem cell therapy.

Here, we have examined the temporal, quantitative, and functional role of BM-derived myofibroblasts in the carbon tetrachloride (CCl<sub>4</sub>) and thioacetamide (TAA)

---

**Abbreviations used in this paper:** α-SMA, α-smooth muscle actin; β-gal, β-galactosidase; BM, bone marrow; CCl<sub>4</sub>, carbon tetrachloride; FISH, fluorescent in situ hybridization; GFAP, glial fibrillary acidic protein; HSC, hematopoietic stem cells; MSC, mesenchymal stem cells; TAA, thioacetamide; ISH, in situ hybridization.

© 2006 by the American Gastroenterological Association Institute  
0016-5085/06/\$32.00  
doi:10.1053/j.gastro.2006.01.036

mouse models of liver fibrosis. We show that, following liver damage, the BM supplies increasing numbers of hepatic stellate cells and myofibroblasts and that these BM-derived hepatic myofibroblasts are of mesenchymal stem cell (MSC) origin and contribute functionally to liver fibrosis. We show that, by altering the source of donor BM used in the transplant experiments, we could modulate the liver's fibrotic response to injury. This suggests that the BM may be a potential therapeutic target in fibrotic diseases affecting the liver and other organs.

## Materials and Methods

### Mouse Models

All animal work was carried out under procedural and ethical guidelines of the British Home Office. To determine the contribution of the BM to hepatic stellate cells and myofibroblasts during the development of cirrhosis, we performed sex mismatched BM transplantations from male donor mice into female recipients; 6-week-old female Balb/c mice received lethal irradiation (8 Gy in a divided dose 4 hours apart) and whole BM transplants from 6-week-old male donors. Mice immediately received a tail vein injection of BM; unless stated, this was  $1 \times 10^6$  whole BM cells isolated from flushing the femur, tibia, and pelvis of male donor mice with a 29-gauge needle containing phosphate-buffered saline (PBS)/2% fetal calf serum (FCS). Mice were placed on acidified water, and, 4 weeks later, mice received intraperitoneal (IP) injections of 1  $\mu$ L per gram body weight of a CCl<sub>4</sub>/olive oil mixture (1:7 ratio, Sigma-Aldrich, Gillingham, United Kingdom) every 5 days. Groups of mice ( $n = 4$  unless stated) were killed at intervals from 0 to 12 weeks of CCl<sub>4</sub>, always at 72 hours following the last injection.

To determine whether BM-derived stellate cells and myofibroblasts were a stable cell population after the recovery of liver injury, BM transplanted mice that had received 8 weeks of CCl<sub>4</sub> were allowed to recover for 8 weeks prior to tissue analysis. A second model of liver damage was also used: female Balb/c mice received male BM transplants as before; 4 weeks later, TAA (Sigma, T-8531) was administered IP at 200 mg/kg body weight (diluted in distilled water) 3 times each week for 4 weeks. Mice receiving TAA ( $n = 8$ ) and controls (no damage,  $n = 4$ ) were killed, and tissue was harvested 3 days after the final dose of TAA.

Cells of BM origin were tracked in liver sections through the use of fluorescent in situ hybridization (FISH) for the Y chromosome. In addition, to confirm the FISH analysis in tissue, male and female control mice and a number of mice that had received BM transplants and 8 weeks of CCl<sub>4</sub> had stellate cells isolated from their livers, using collagenase and pronase digestion followed by density centrifugation.<sup>25</sup> FISH was performed on the isolated stellate cells.

To assess whether the BM-derived hepatic myofibroblasts were capable of intrahepatic collagen transcription, 6-week-old

female C57/B6 mice (after 10 Gy irradiation in a divided dose 4 hours apart) underwent transplantation with whole BM from 6-week-old male Col1a2 mice that express the  $\beta$ -galactosidase ( $\beta$ -gal) reporter gene under control of the  $\alpha$ 2(I) collagen gene enhancer, giving a direct assay of transcriptional activity for collagen type I.<sup>26</sup> This mouse model activates the transgene following CCl<sub>4</sub> injury.<sup>27</sup> Control mice received BM transplants from C57/B6 mice; all mice received 12 weeks of CCl<sub>4</sub>.

To analyze whether BM-derived myofibroblasts can determine the fibrotic phenotype in liver injury, C57/B6 mice received BM transplants from Col 1a1<sup>rr</sup> mice ( $n = 4$ ). These mice have mutated collagen, which is collagenase resistant, and, when their livers are injured by CCl<sub>4</sub>, the mice develop extensive pericellular fibrosis.<sup>28</sup> Control mice received BM transplants from C57/B6 mice ( $n = 4$ ); all mice received 8 weeks of CCl<sub>4</sub> and were killed 1 week following the final injection.

To determine whether the hepatic myofibroblasts were of MSC or hematopoietic stem cell (HSC) origin, 6-week-old female Balb/c mice were lethally irradiated and received BM from donor mice as follows: Group 1 received injections of  $1.2 \times 10^6$  enriched female MSCs and  $2.3 \times 10^5$  enriched male HSCs ( $n = 3$ ). Group 2 received injections of  $1.2 \times 10^6$  enriched male MSCs and  $2.3 \times 10^5$  enriched female HSCs ( $n = 3$ ). All mice received 6 weeks of CCl<sub>4</sub>. The contribution of each BM stem cell fraction to hepatic myofibroblast populations was assessed by performing immunohistochemistry for  $\alpha$ -smooth muscle actin ( $\alpha$ -SMA) together with FISH for the Y chromosome.

### MSC Enrichment

We used Balb/c mice aged 4–6 weeks. Mice were killed by cervical dislocation at the time of BM harvest. BM cells were extracted from the tibia and femur by flushing with culture medium using a 10-mL syringe and a 29-gauge needle. The cells were then passed through a 70-mm nylon mesh and were washed 3 times with PBS containing 2% FCS. Next, cell numbers were counted using a hemocytometer, and cell viability was determined using trypan blue staining. The cells were plated at a density of  $7 \times 10^7$  per 150-cm<sup>2</sup> tissue culture flask and cultured for 1 week in MSC culture medium (MesenCult medium plus Mesenchymal Stem Cell stimulatory supplements; Stem Cell Technologies, Vancouver, Canada) at 37°C in a humidified atmosphere of 5% CO<sub>2</sub> and 95% air. The culture medium was replaced twice a week to remove the nonadherent cells. Next, the adherent cells thus obtained were trypsinized (0.05% trypsin and 0.53 mmol/L EDTA; Gibco BRL), washed, and used for the experiments. Each recipient received  $1.2 \times 10^6$  MSCs via tail vein injection.<sup>29</sup>

### HSC Enrichment

For HSC isolation and characterization, mouse BM was obtained by flushing femoral, tibial, and pelvic bones with a 29-gauge needle containing cold PBS/2% FCS. After red blood cell lysis, the BM cells were counted using a hemocytometer, and cell viability was determined using trypan blue staining,

and then washed before double lineage depletion by using the standard immunomagnetic StemSep protocol (StemSep Murine Kit; StemCell Technologies) according to manufacturer's instruction.<sup>30</sup> The antibodies used were against mouse CD5 (clone Ly-1), myeloid differentiation antigen (Gr-1), CD45R (B220), erythroid cells (TER119), CD11b (Mac-1), and neutrophils (7-4) (Stem Cell Technologies). Each recipient received  $2.3 \times 10^5$  double lineage-depleted HSCs via tail vein injection.

### Tissue Analysis: Collagen Staining and Immunohistochemistry

Sirius red (BDH Laboratory Supplies, Poole, Dorset, England) staining was performed to identify collagen. To identify stellate cells, sections were immunostained for glial fibrillary acidic protein (GFAP; polyclonal rabbit, Z 0334, DAKO Cytomation Ltd, Cambridgeshire, United Kingdom) or desmin (monoclonal mouse anti-human desmin, M0760, DAKO). To identify activated myofibroblasts, sections were immunostained for  $\alpha$ -SMA (mouse monoclonal Clone 1A4, A-2547, Sigma, Poole, United Kingdom). To detect  $\beta$ -gal, a rabbit anti- $\beta$ -gal antibody (ab 616, Abcam Ltd, Cambridge, United Kingdom) was used. Five-micrometer-thick sections were dewaxed and, when peroxidase detection was used, slides were incubated with hydrogen peroxide (1.8%) in methanol, taken through graded alcohol to PBS, and microwaved for 5 to 10 minutes in sodium citrate (2.94 g/L). For GFAP detection, the slides were also digested with trypsin for 20 minutes at room temperature. A biotin-blocking step was used (DAKO X0590). Slides were preincubated in normal rabbit or swine serum (DAKO D0396) at 1:25 dilution in PBS for 10 minutes. The slides were then incubated in primary antibody ( $\alpha$ -SMA, GFAP, or  $\beta$ -gal) at a dilution of 1:4000, 1:500, and 1:500, respectively, in PBS (35 minutes at room temperature for  $\alpha$ -SMA and GFAP detection and overnight at 4°C for  $\beta$ -gal detection). The secondary antibody was a biotinylated rabbit anti-mouse (DAKO, E0354) for  $\alpha$ -SMA and biotinylated swine anti-rabbit (DAKO E353) for GFAP and  $\beta$ -gal detection, applied for 35 minutes at room temperature. A tertiary layer of either streptavidin-alkaline phosphatase (AP) (DAKO D0396) diluted to 1:50 in PBS or streptavidin-horseradish peroxidase (HRP) (DAKO P0397) diluted to 1:500 in PBS was used for 35 minutes at room temperature. Sections were washed in PBS between each antibody layer and developed in Vector Red substrate (Vector Laboratories SK 5100, Peterborough, United Kingdom) or DAB substrate (Sigma D 5637).

For  $\alpha$ -SMA immunohistochemistry prior to FISH for the both the X and Y chromosomes, the sections were washed in PBS and then incubated with Cy5-labelled goat anti-rabbit IgG (Cambridge BioScience 81-6116, Cambridge, United Kingdom) diluted to 1:100. Sections were again washed in PBS prior to the FISH protocol. All antibodies (ab) were diluted in PBS except for the anti  $\beta$ -gal ab, which was diluted 1:500 in PBS + 1% BSA + 0.1% Tween 20 + 0.1 mmol/L  $\text{CaCl}_2$ .

### Tissue Analysis: In Situ Hybridization

The BM origin of myofibroblasts was confirmed by FISH for the Y chromosome (STARFISH 1189-YMF; Cambio, Cambridge, United Kingdom). To determine the chromosomal complement of the cells with a myofibroblast phenotype, we performed FISH for both X (Cy3 labelled, STARFISH, 1200-MCy3, Cambio) and Y (FITC labelled, STARFISH, 1189-YMF, Cambio) chromosomes, combined with immunohistochemistry for  $\alpha$ -SMA using an indirectly labelled Cy5 signal. Each myofibroblast nucleus was analyzed using confocal microscopy for the number of signals from the X and Y chromosomes. Sections were incubated in 1 mol/L sodium thiocyanate for 10 minutes at 80°C, washed in PBS, and digested in pepsin (0.4% wt/vol) in 0.1 mol/L HCl at 37°C for 12 minutes. The protease was quenched in glycine (0.2% vol/wt) in double-concentration PBS, and the sections were then rinsed in PBS, postfixed in paraformaldehyde (4% wt/vol) in PBS, dehydrated through graded alcohols, and air-dried. The chromosome paints were used in the supplier's hybridization mix, added to the sections, sealed under glass with rubber cement, heated to 60°C–80°C for 10 minutes, and incubated overnight at 37°C. The slides were rinsed in  $0.5 \times \text{SSC}$  and then PBS. The slides were mounted in Vectashield (Vector Laboratories), except when sections that were immunostained with the Cy5-labelled antibody (when Citifluor mounting was used) and when slides that were processed for in situ hybridization (ISH) for the Y chromosome probe combined with ISH for pro( $\alpha$ 1)I collagen messenger RNA (mRNA) where the pre-treatments were extensively modified. Then the slides were washed with PBS and incubated with 1:250 peroxidase-conjugated antifluorescein antibody (150 U/mL; Boehringer Mannheim; Indianapolis, IN; <http://www.roche-applied-science.com>) for 60 minutes at room temperature and developed in DAB substrate. mRNA for pro( $\alpha$ 1)I was located by ISH using an antisense riboprobe synthesised with T3 RNA polymerase using [ $^3\text{H}$ ]-UTP ( $\sim 800$  Ci/mmol; Amersham PLC, Buckinghamshire, UK) and plasmid prepared from I.M.A.G.E. consortium Clone I.D. 335137 linearized with *Eco*RI to yield an antisense probe, which was used without hydrolysis. The region of sequence used to produce the riboprobe did not show significant homology to any other known gene sequences in the database. [ $^3\text{H}$ ]-UTP decays releasing low-energy particles (0.018 MeV) and hence improves spatial resolution (0.5–1.0  $\mu\text{m}$ ) compared with  $^{35}\text{S}$ . Slides were pretreated with Proteinase K (Sigma P4914: 20 mg/mL in prewarmed PBS for 10 minutes). The presence of hybridizable mRNA in all compartments of the tissues studied was established in near serial sections using an antisense  $\beta$ -actin probe. Autoradiography was at 4°C, before developing in Kodak D19 and counterstaining with hematoxylin. Sections were examined under conventional light microscopy that allowed individual autoradiographic silver grains to be seen as black spots and the Y probe as a nuclear peroxidase label.

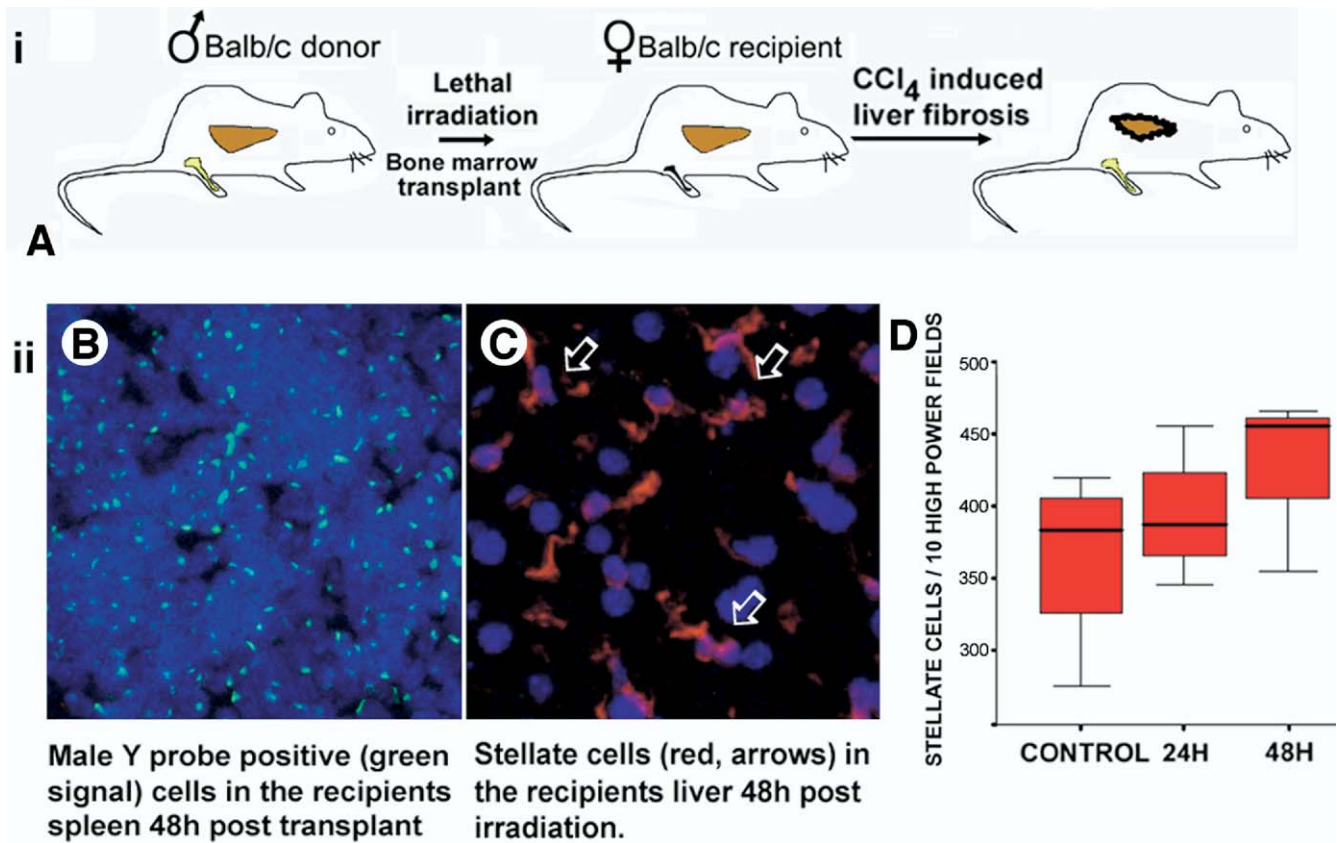


**Figure 1.** (A) Female Balb/c mice received whole BM transplants at the age of 6 weeks from 6-week-old male Balb/c donor mice. From 4 weeks post-irradiation groups of mice received CCl<sub>4</sub> injections to induce cirrhosis. Control mice received no liver damage. (B–D) To confirm that hematopoietic reconstitution from the donor mouse had occurred, spleens were routinely analyzed for the Y chromosome (B). Here, we can see that, even at 1 week, the cells are of donor (male) origin (original magnification,  $\times 400$ ). To confirm that the irradiation protocol does not deplete stellate cells were analyzed within the liver, these were analyzed in liver sections using GFAP immunohistochemistry; (C) stellate cells were readily detected in the livers of irradiated mice at 24 and 48 hours following irradiation (original magnification,  $\times 400$ ); (D) quantification revealed no loss in the number of stellate cells in irradiated mice compared with controls ( $n = 4$  per group).

### Microscopy and Image Capture

For light microscopy, a Nikon Eclipse E600 microscope (Nikon UK Ltd., Surrey, UK) was used with a DXM 1200F digital camera. For fluorescent microscopy, slides were visualized using a Zeiss Axioplan 2 fluorescence microscope (Carl Zeiss UK Ltd., Hertfordshire, UK) equipped with a triple bandpass filter. Gray-scale images were collected with a cooled charge-coupled device camera (Quantix Corporation, Cambridge, MA) and analyzed using Mastercapture software. For confocal microscopy, a Zeiss Axiovert 200 M microscope equipped with a triple bandpass filter was used; images were collected with a CCD camera and analyzed with Zeiss LSM Image Browser software. Image processing was performed using Adobe Photoshop software (Adobe Systems UK, Uxbridge, Middlesex, UK).

### Cell Counting

To document the myofibroblast response of the liver to damage, we analyzed tissue by immunostaining for the myofibroblast marker  $\alpha$ -SMA combined with FISH for the Y chromosome. For each mouse liver, sections were analyzed by digitally photo-

graphing 10 consecutive sections at  $\times 400$  total magnification. The number of myofibroblasts in each field and the proportion of BM-derived (Y chromosome positive) myofibroblasts was quantified. Five-micrometer-thick tissue sections may result in the X and Y chromosome being missed and, therefore, a correction factor was determined.<sup>31</sup> Five male mice received 12 weeks of CCl<sub>4</sub> treatment then the proportion of hepatic myofibroblasts in which the Y chromosome could be detected was counted and found to be 62.3% ( $n = 5$ ). Therefore, absolute chromosome counts were divided by 0.623 to give corrected counts, which are presented throughout. To determine the X and Y chromosomal ratios within Y chromosome-positive hepatic myofibroblasts, liver tissue was analyzed from mice that had received 12 weeks of CCl<sub>4</sub> treatment, with X and Y chromosome detection combined with immunohistochemistry for  $\alpha$ -SMA. For each animal, 10 random myofibroblasts were selected in which the nucleus was within the tissue section as observed by confocal microscopy. Using “z-stack” scanning through the nucleus, evidence for multiple X and Y chromosomes within myofibroblast nuclei was sought. Results throughout the text are expressed as median (range,  $n =$  number/group).

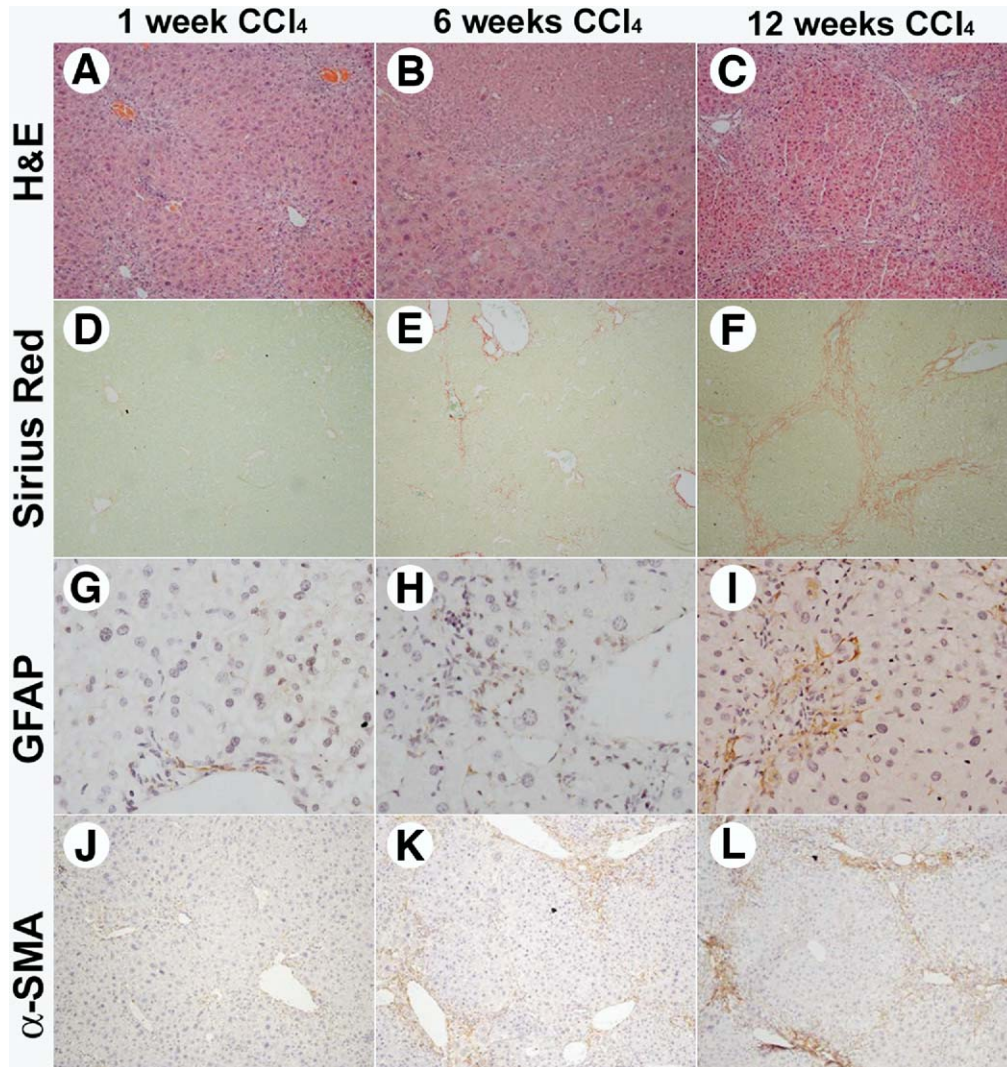


**Figure 2.** Photomicrographs of livers from female Balb/c mice that had received BM transplants from male donor mice, and 4 weeks later, the mice received CCl<sub>4</sub> injections for 12 weeks to induce cirrhosis. *Column 1* shows liver after 1 week of CCl<sub>4</sub> (A, D, G, J). *Column 2* shows liver after 6 weeks CCl<sub>4</sub> (B, E, H, K). *Column 3* shows liver after 12 weeks CCl<sub>4</sub> (C, F, I, L). H&E-stained sections show the developing liver damage with nodules (A–C). Collagen staining (Sirius red) demonstrates the formation of extensive collagen in the livers over the 12-week period (D–F) (original magnification, ×100). Immunostaining for stellate cells (GFAP, brown) shows the location of stellate cells predominantly in the areas of tissue damage (G–I) (original magnification, ×400). Immunostaining for myofibroblasts (α-SMA, brown) shows the increasing number of myofibroblasts with increasing tissue damage; these myofibroblasts are in the area of scarring surrounding the nodules (J–L) (original magnification, ×200).

**Results**

We confirmed that, following lethal irradiation and BM transplantation, hematologic reconstitution was complete: the spleens of all the female recipient mice showed reconstitution by male cells (Figure 1B). We confirmed that the indigenous stellate cells in the recipient mice were not damaged by the irradiation; stellate cells (red) can be seen in the liver of a mouse 48 hours following lethal irradiation, and total numbers of stellate cells were quantified in groups of mice at 0, 24, and 48 hours after irradiation, which confirmed no depletion of stellate cell numbers. We therefore concluded that the

irradiation and transplant model was valid and reflected the situation in nonirradiated nontransplanted mice.

Following transplantation initially, there were no stellate cells of BM origin at 1 week (n = 4) and 2 weeks (n = 4); however, stellate cells of BM origin could be detected by 4 weeks post-BM transplantation, at a frequency of 14.4% (range, 2; n = 4); the proportion of BM-derived stellate cells remained steady in the absence of liver damage with 13% (range, 15; n = 4) at 8 weeks post-BM transplantation.

We then sought to assess the role of the BM in the damaged liver. Cirrhosis was induced by the administra-

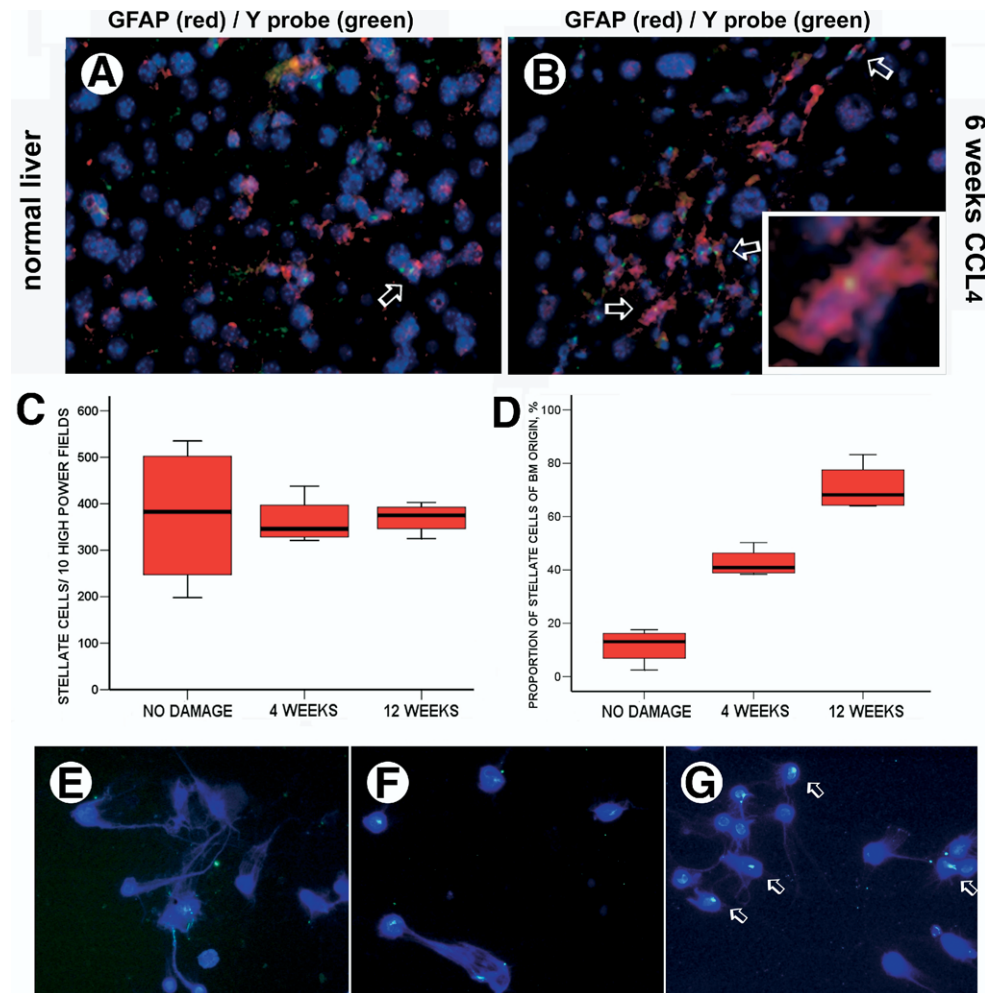


**Figure 3.** (A–G) Photomicrographs of livers from female mice that have received male BM transplants. (A) In undamaged liver, scattered GFAP-positive (*red*) stellate cells can be seen; only a few of these cells contain signals for the Y chromosome (*green*, *arrow*). (B) Liver from an animal that received 6 weeks of CCl<sub>4</sub>; in the areas of scarring, there are GFAP-positive (*red*) stellate cells that are frequently positive for the Y chromosome (original magnification,  $\times 400$ ). (C) The total numbers of GFAP-positive stellate cells and (D) the proportion of stellate cells from the BM seen during the development of cirrhosis (compared with animals without liver damage at 8 weeks post-BM transplant). To confirm the tissue analysis, stellate cells were isolated from the livers of mice that had received 8 weeks CCl<sub>4</sub>. (E) In female mice, the cells are Y chromosome negative (F). In male mice, the stellate cells contain the Y chromosome (*green spot*); and (G) in female mice that received male BM transplants prior to liver damage, the stellate cells often contained the Y chromosome (*green spots*, *arrows*) (original magnification,  $\times 400$ ).

tion of CCl<sub>4</sub> over 12 weeks. Hepatic nodules (Figure 2A–C) and bridging fibrosis developed in all livers, indicated by an increase in intrahepatic collagen staining (Figure 2D–F). The total numbers of GFAP-positive stellate cells remained constant during the development of cirrhosis with 383 (range, 337;  $n = 4$ ) cells/unit area in the undamaged liver and 375 (range, 78;  $n = 4$ ) cells/unit area after 12 weeks of administration of CCl<sub>4</sub> (Figure 3C). In the undamaged liver, stellate cells were evenly distributed throughout the liver, but, by 12 weeks of CCl<sub>4</sub>, stellate cells were found predominantly in the areas of scarring (Figure 2I). Over the 12 weeks of liver damage, the proportion of stellate cells from the BM increased markedly to 68% (range, 19;  $n = 4$ ) by 12 weeks of liver damage, suggesting an axis of renewal

from the BM (Figure 3D). In contrast, the total number of  $\alpha$ -SMA-positive myofibroblasts/unit area increased in all mice receiving CCl<sub>4</sub>. In the undamaged liver, no  $\alpha$ -SMA-positive myofibroblasts were identified that were not associated with hepatic vessels or the liver capsule. Following 1 week of liver injury, there were 120 (range, 121;  $n = 4$ ) myofibroblasts/unit area, which increased to 349 (range, 481;  $n = 4$ ) myofibroblasts/unit area after 12 weeks of CCl<sub>4</sub> (Figure 3L). The myofibroblasts were found in the areas of scarring, and, by 12 weeks, they surrounded the hepatic nodules. The proportion of myofibroblasts of BM origin remained constant during the development of liver fibrosis, being 69% (range, 22;  $n = 4$ ) at week 1 and 69% (range, 8;  $n = 4$ ) at week 12 (Figure 3M). After only 1 week of liver damage, 67.8%

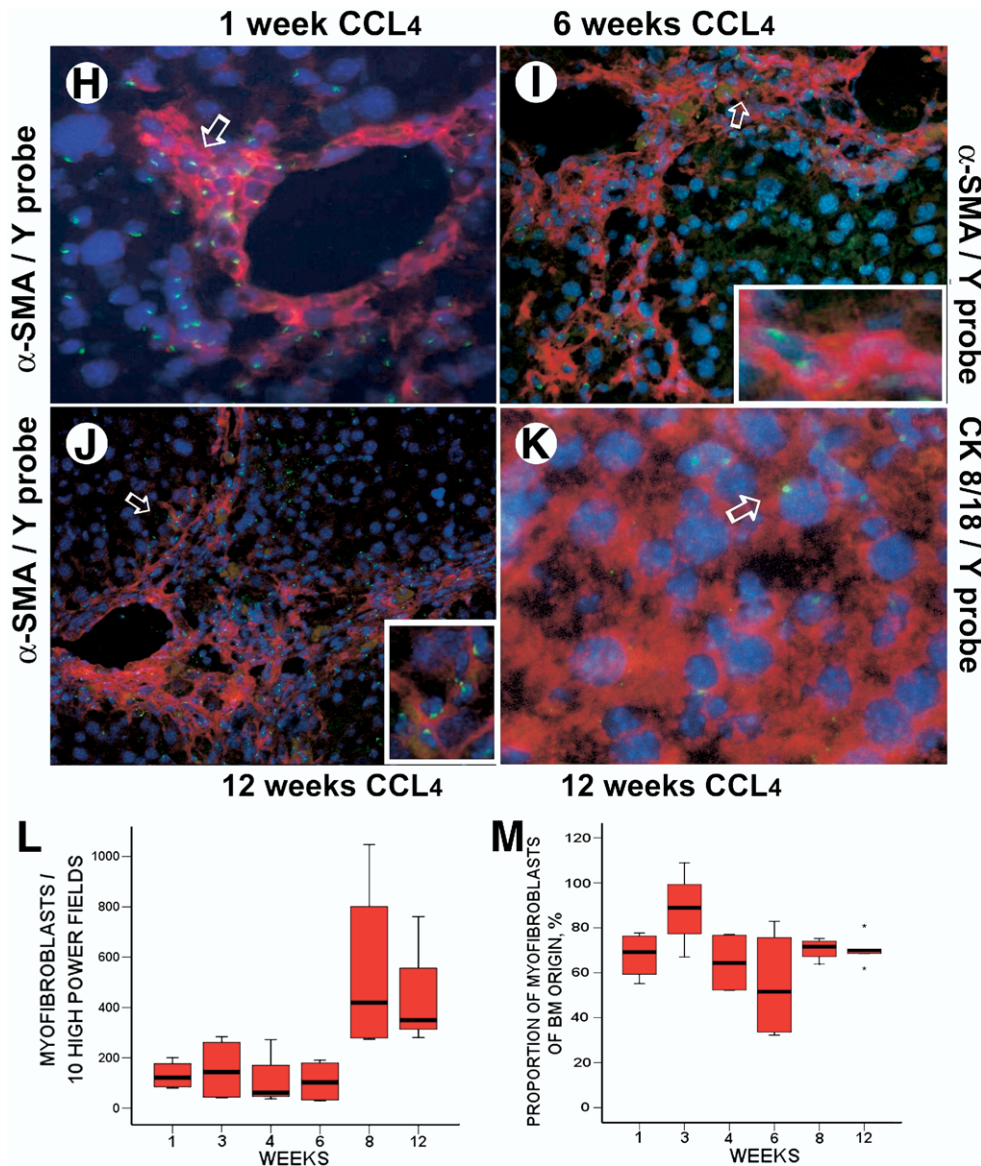


**Figure 3 (cont).** (H–M) Photomicrographs of female mouse livers that have received whole male BM transplants followed by CCl<sub>4</sub> injections for 1–12 weeks;  $\alpha$ -SMA-positive myofibroblasts (red) can be seen that contain the Y chromosome (green, arrows). (H) These cells are seen in small groups following 1 week of liver damage and (I) are seen in areas of developing scars by 6 weeks of liver injury (arrows and enlarged box) (original magnification,  $\times 400$ ). (J) After 12 weeks of CCl<sub>4</sub>, the myofibroblasts are in dense bands associated with the collagen scars surrounding the regenerative nodules (arrows) (original magnification,  $\times 200$ ). (K) Occasional cytokeratin 8/18-positive hepatocytes were identified with single Y chromosome nuclear signals (arrow) (original magnification,  $\times 600$ ). (L) The total hepatic myofibroblast density ( $\alpha$ -SMA-positive cells) increases significantly during the development of cirrhosis. (M) The proportion of myofibroblasts from the BM remains relatively constant throughout the development of cirrhosis. Figure shows median values (line), interquartile range (boxes), and range (whiskers).

of the hepatic myofibroblasts were of BM origin, and this remained unchanged during the formation of cirrhosis. At this time, only 11.6% of the stellate cells were BM derived (1 week of liver injury). This could indicate 2 or more sources of BM-derived hepatic myofibroblasts: first, a path via the hepatic stellate cells and, second, a direct pathway from the BM. An alternative explanation for these findings could be that BM-derived stellate cells are preferentially activated in liver injury.

We sought evidence of “BM-derived” hepatocytes. In mice that had received 12 weeks of CCl<sub>4</sub>, only 0.6% (range, 0.8; n = 7) of hepatocytes had nuclear Y chromosome signals; in control animals with no liver damage (sham CCl<sub>4</sub> for 12 weeks), no Y chromosome-positive hepatocytes were found (n = 5). We only found single Y chromosome signals in the positive hepatocyte nuclei, (Figure 3K) in contrast to the X chromosome signals, which were invariably multiple. This apparent imbalance



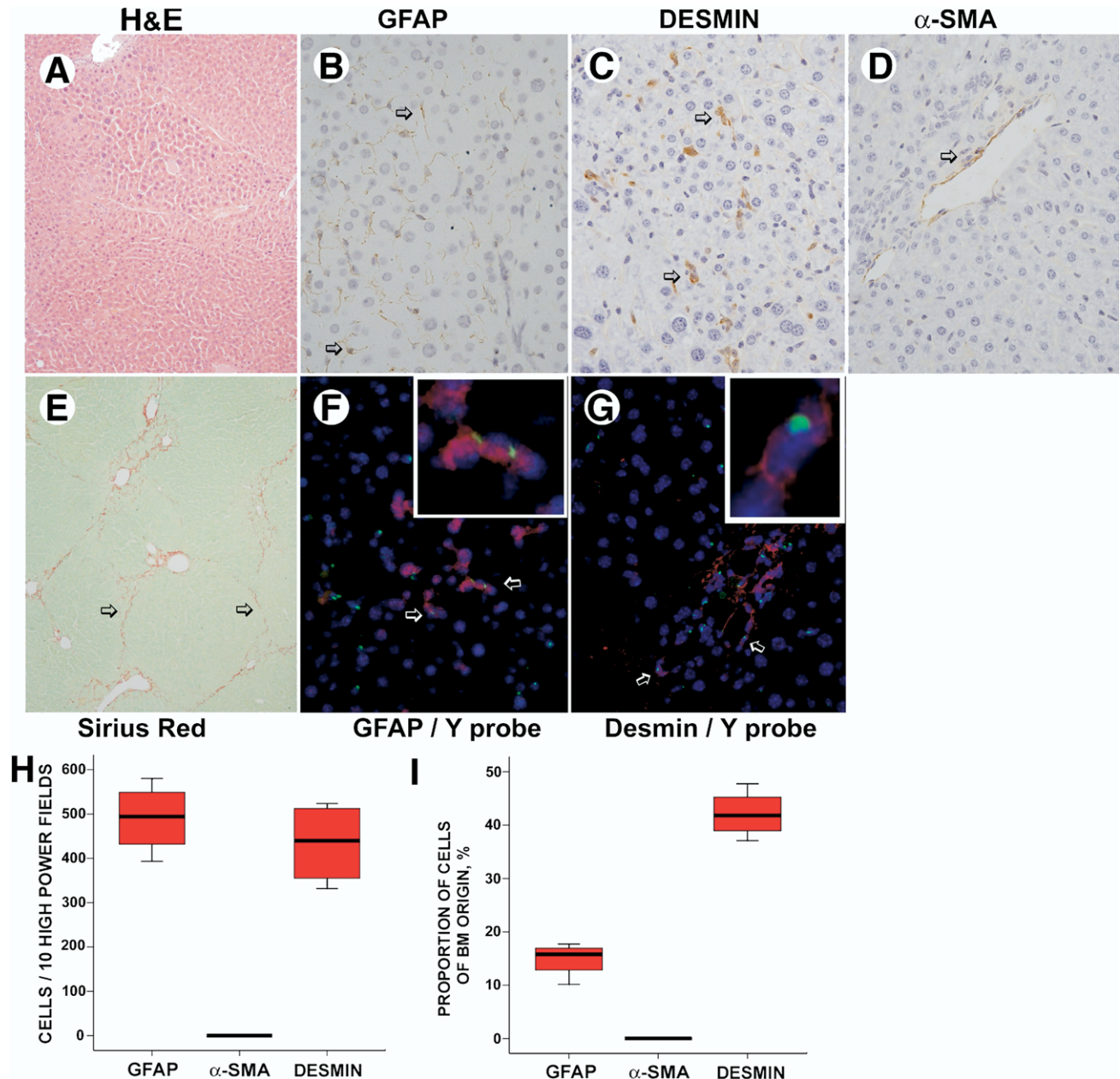


**Figure 4.** The stability of the BM-derived stellate cells and myofibroblasts in a liver injury-recovery model. Six-week-old female mice received whole male BM transplants from 6-week-old male donor mice. Four weeks later, the mice received  $\text{CCl}_4$  injections every 5 days for 8 weeks. Mice were allowed to recover for 8 weeks and then killed and the livers analyzed. (A) H&E-stained sections show only minimal nodularity within the liver (original magnification,  $\times 100$ ). (B) Stellate cells (GFAP, brown) are seen throughout the liver parenchyma (arrows) (original magnification,  $\times 200$ ). (C) Desmin-positive myofibroblasts (brown, arrows) were located predominantly in areas of tissue damage (original magnification,  $\times 200$ ). (D)  $\alpha$ -SMA-positive cells (brown) were found only in association with the hepatic vessels (original magnification,  $\times 200$ ). (E) Collagen staining (red) demonstrates the presence of thin residual collagen bands in the livers (original magnification,  $\times 100$ ). (F) GFAP-positive stellate cells (red) can be seen that contain the Y chromosome (green) (original magnification,  $\times 400$ ). (G) Desmin-positive cells (red) can be seen that contain the Y chromosome (green) (original magnification,  $\times 400$ ). (H and I) The numbers of stellate cells/myofibroblasts per 10 high-power fields and the proportions of stellate cells/myofibroblasts of BM origin following the recovery from injury for each cell phenotype. Figure shows median values (line), interquartile range (boxes), and range (whiskers).

would be in keeping with a cell fusion event between a BM-derived cell and a polyploid hepatocyte, although this was not formally assessed because 5- $\mu\text{m}$  tissue sections do not include the whole of the hepatocyte nucleus.

Following 8 weeks recovery, the livers had only minimal nodularity and fine residual collagen bands (Figure 4A and E). GFAP-positive stellate cells were distributed evenly throughout the liver parenchyma, and, again, the

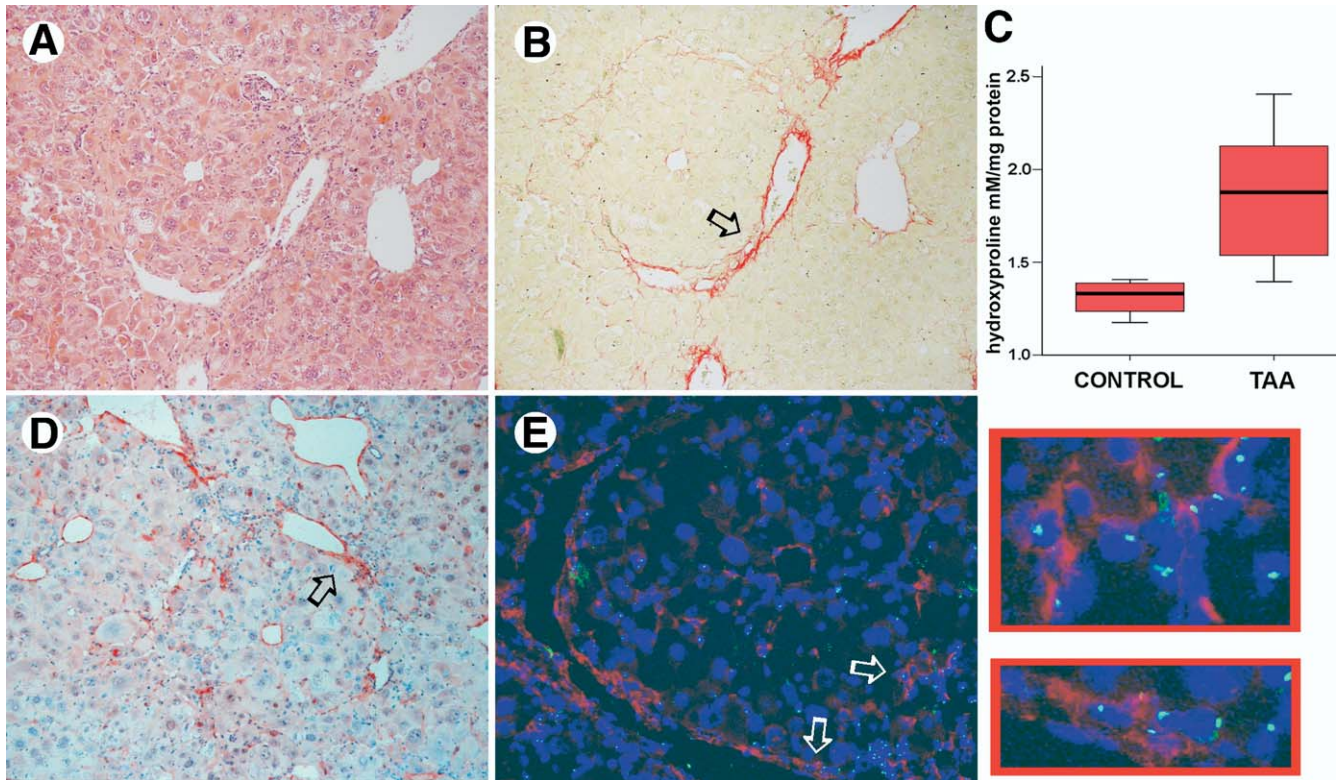


**Figure 5.** A second model of liver fibrosis was used to induce liver damage (4 weeks TAA) in female mice that had previously received male BM transplants. (A) H&E staining shows the early development of hepatic nodularity (original magnification,  $\times 200$ ); (B) collagen staining (Sirius red) shows the development of collagen bands (arrows) (original magnification,  $\times 200$ ), and (C) hepatic hydroxyproline is increased over control (undamaged) mice. (D)  $\alpha$ -SMA-positive myfibroblasts are seen in the liver (red, arrows) (original magnification,  $\times 200$ ); (E) these hepatic myfibroblasts were frequently of BM origin (Y probe positive, green, arrows [original magnification,  $\times 400$ ] and enlarged examples in red boxes).

total numbers of stellate cells/unit area remained constant (Figure 4B). The proportion of stellate cells of BM origin fell to 16% (range, 8;  $n = 4$ ), suggesting an intrahepatic source of renewal. The only  $\alpha$ -SMA-positive cells seen in these livers were associated with vessels (Figure 4D). We did, however, identify a population of desmin-positive cells (Figure 4C) that were predominantly found in areas of residual scarring, and 42% (range, 11;  $n = 4$ ) of these cells were of BM origin (Figure 4I). These results suggest that the hepatic stellate cell-myfibroblast populations are heterogeneous in origin and phenotype and that both intrahepatic and BM-derived sources are important in the development of fibrosis.

To confirm the importance of the BM in supplying myfibroblasts to the damaged liver, another model of liver injury was tested (TAA). Here, we confirmed in our BM transplant model that, following 4 weeks of TAA, there was an increase in hepatic collagen and parenchymal myfibroblasts (Figure 5); again following 4 weeks damage, the hepatic myfibroblasts were frequently found to be of BM origin at 33.9% (range, 7;  $n = 8$ ).

We sought to define the *functionality* of the BM-derived myfibroblasts. We found  $\beta$ -gal-positive cells in

the areas of liver scarring in mice that had received BM from Col1a2 mice but not in mice that had received wild-type BM (Figure 6A and B). When  $\beta$ -gal immunostaining was combined with FISH for the Y chromosome, this confirmed that the  $\beta$ -gal-positive cells were of BM origin (Figure 6C and D), indicating that the BM-derived myfibroblasts were transcriptionally active for collagen type 1. These  $\beta$ -gal-positive cells were slightly less common at 161.5 cells/unit area (range, 110;  $n = 6$ ) compared with the absolute numbers of BM-derived  $\alpha$ -SMA-positive myfibroblasts seen at 226.3 cells/unit area (range, 87;  $n = 6$ ), which may indicate that not all myfibroblasts are actively transcribing collagen at a single time point. We also assessed collagen transcription using an independent technique: we performed ISH for mRNA for pro( $\alpha 1$ )I collagen together with FISH for the Y chromosome and immunohistochemistry for  $\alpha$ -SMA in livers from the female mice that received male BM transplants and 12 weeks CCl<sub>4</sub>. We again identified collagen transcription in the scar areas of liver that could be localized to BM-derived myfibroblasts (Figure 6E and F).

Mice that received BM from the Col 1a1<sup>fl</sup> mice developed extensive and characteristic pericellular fibrosis

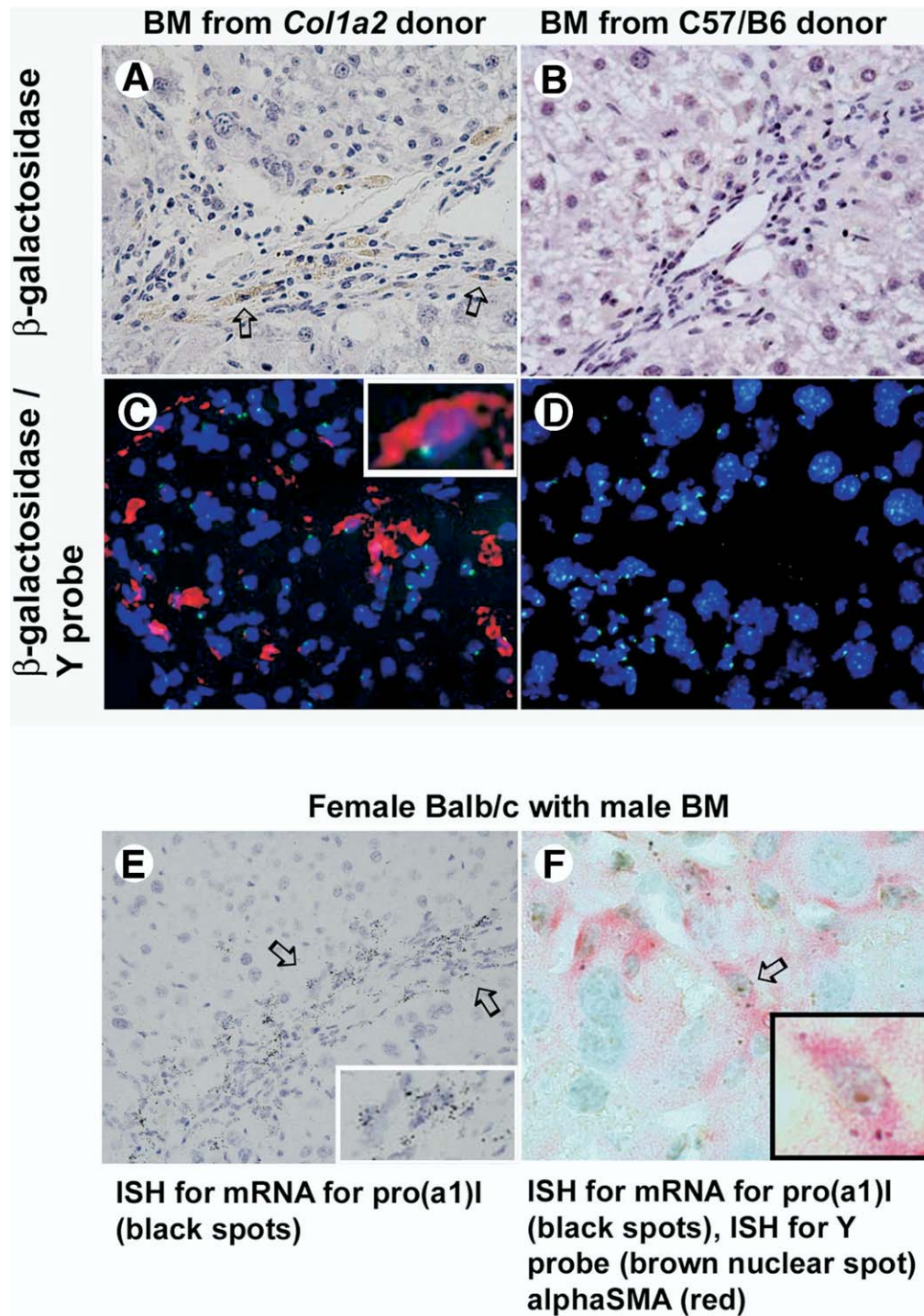


**Figure 6.** To assess whether the BM-derived myfibroblasts are active for collagen transcription, we performed BM transplants into C57/B6 mice from *Col1a2* mice. These mice express the β-gal reporter gene under control of the α2(I) collagen gene enhancer *Col1a2*. Four weeks later, the mice received CCl<sub>4</sub> for 12 weeks. Photomicrographs of liver from female C57/B6 mice that had received BM transplants from either (A and C) male *Col1a2* mice or (B and D) male C57/B6 mice and then received 12 weeks of CCl<sub>4</sub>. (A and B) Sections have been immunostained for β-gal (brown), indicating that collagen transcription from BM-derived cells is seen in the mice that received BM from the *Col1a2* mice. No β-gal immunopositivity is seen in the control mice that were transplanted with wild-type BM. (C and D) Sections have been immunostained for β-gal with alkaline phosphatase detection (red) followed by FISH for the Y chromosome. The mice receiving BM from the *Col1a2* donor mice have β-gal positive (red) cells associated with areas of scarring that are positive for the Y chromosome (green) confirming that the cells producing collagen (β-gal positive) are from the BM. Control mice have BM-derived cells in areas of scarring but have no β-gal immunopositivity (original magnification, ×400). Using an independent technique, we assessed collagen transcription in livers from the female mice that have received whole male BM transplants and 12 weeks CCl<sub>4</sub>. Sections were processed using ISH for mRNA for pro(α1)I. (E) This revealed active collagen transcription in the scar areas of liver (black spots, arrows). (F) When this was combined with ISH for the Y chromosome and α-SMA immunostaining, we identified BM-derived (peroxidase brown nuclear signal) myfibroblasts (red) that were active for collagen transcription (black spots, arrows, and enlarged cell in the inset) (original magnification, ×600).

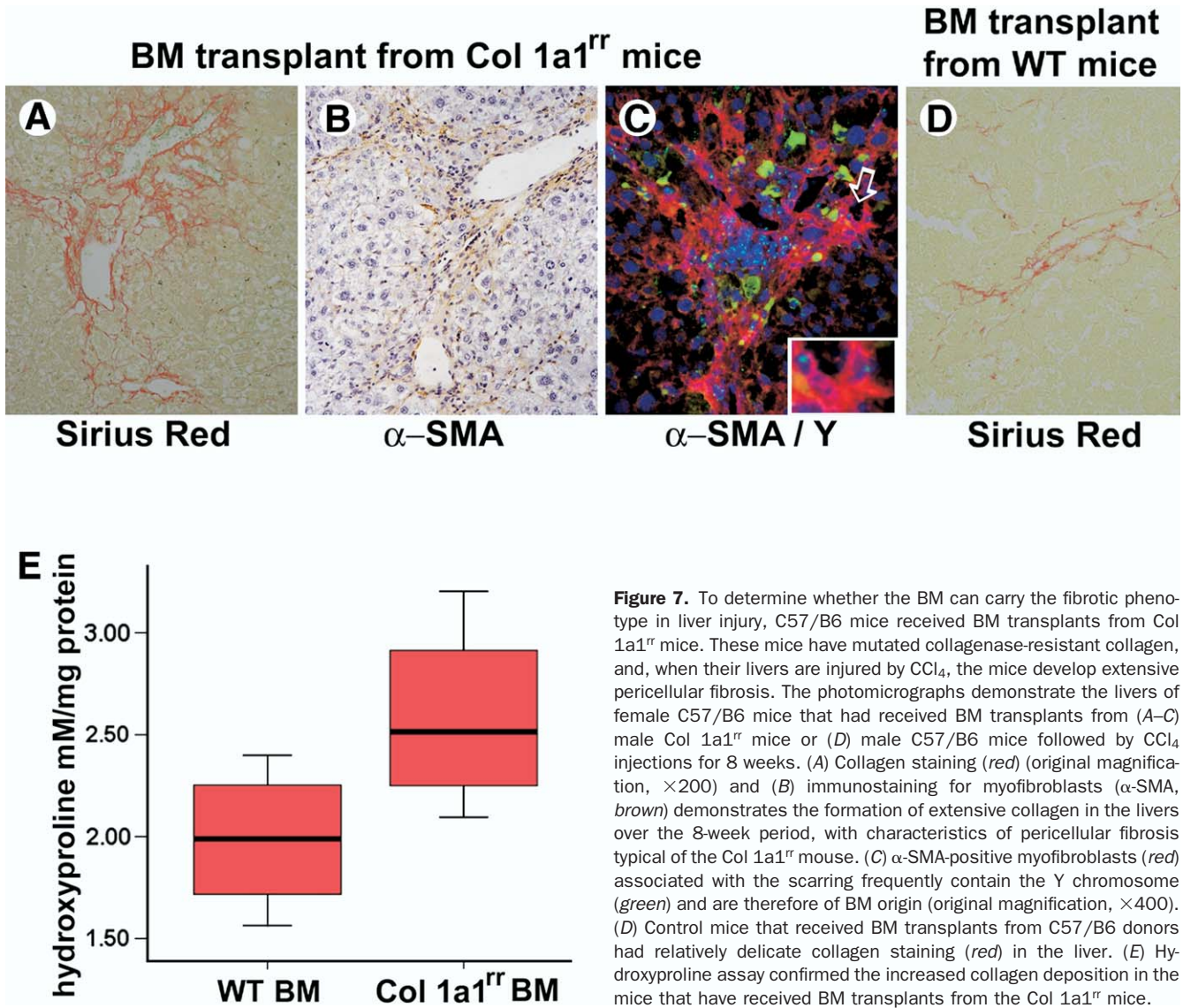


**Figure 7.** To determine whether the BM can carry the fibrotic phenotype in liver injury, C57/B6 mice received BM transplants from Col 1a1<sup>rr</sup> mice. These mice have mutated collagenase-resistant collagen, and, when their livers are injured by CCl<sub>4</sub>, the mice develop extensive pericellular fibrosis. The photomicrographs demonstrate the livers of female C57/B6 mice that had received BM transplants from (A–C) male Col 1a1<sup>rr</sup> mice or (D) male C57/B6 mice followed by CCl<sub>4</sub> injections for 8 weeks. (A) Collagen staining (red) (original magnification, ×200) and (B) immunostaining for myofibroblasts (α-SMA, brown) demonstrates the formation of extensive collagen in the livers over the 8-week period, with characteristics of pericellular fibrosis typical of the Col 1a1<sup>rr</sup> mouse. (C) α-SMA-positive myofibroblasts (red) associated with the scarring frequently contain the Y chromosome (green) and are therefore of BM origin (original magnification, ×400). (D) Control mice that received BM transplants from C57/B6 donors had relatively delicate collagen staining (red) in the liver. (E) Hydroxyproline assay confirmed the increased collagen deposition in the mice that have received BM transplants from the Col 1a1<sup>rr</sup> mice.

typical of the Col 1a1<sup>rr</sup> mouse, unlike control mice that had more restricted linear collagen deposition with less pericellular collagen (Figure 7A and D). Hydroxyproline quantification in the 2 groups revealed that the mice receiving the mutant BM transplants had a higher level of hepatic hydroxyproline (Figure 7E). The myofibroblasts seen within these areas of scarring were BM derived (Figure 7C); the total proportion of myofibroblasts of BM origin was 63% (range, 8; n = 4) in the mice receiving BM from the Col 1a1<sup>rr</sup> mice and 48.9% (range, 8; n = 4) in the mice receiving BM from the C57/B6 mice. This suggests that the genotype of the BM-derived myofibroblasts can influence the injured organ’s fibrotic response and indicates that the BM is a potential therapeutic target in organ fibrosis.

We sought evidence of cell fusion between BM-derived cells and stellate cells/myofibroblasts because fusion

can result in BM “derived” hepatocytes.<sup>32</sup> Cirrhotic liver tissue from the sex mismatched BM transplant experiments was analyzed by confocal microscopy for X and Y chromosomes (10 myofibroblast nuclei per section in the 4 cirrhotic livers) in combination with immunohistochemistry for α-SMA; in no case was a chromosome pattern indicative of cell fusion (eg, XXXY) seen within a myofibroblast nucleus. We identified only single X and Y chromosomes within myofibroblast nuclei, whereas multiple X chromosome signals were seen in adjacent hepatocyte nuclei (Figure 8A–D). Although the lack of multiple or imbalanced X and Y chromosomes does not definitively rule out cell fusion, cells found arising from fusion between BM-derived cells and indigenous hepatocytes have multiple unbalanced chromosome copies.<sup>33</sup>

In the mice that received BM enriched for male MSCs, 53% (range, 13; n = 3) of myofibroblasts contained the Y

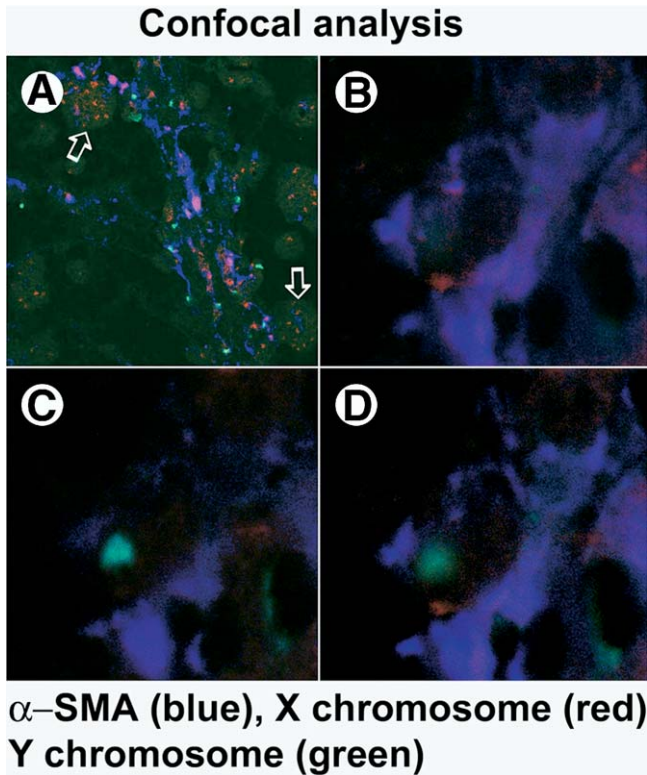


**Figure 8.** Confocal tissue analysis to seek evidence of cell fusion between BM cells and intrinsic hepatic myofibroblasts. Female mice received whole BM transplants at the age of 6 weeks from 6-week-old male donor mice and 4 weeks later received CCl<sub>4</sub> injections every 5 days for 12 weeks. Photomicrographs of liver that have been immunostained for  $\alpha$ -SMA (blue) followed by FISH for the detection of Y (green) and X (red) chromosomes. (A) Multiple X signals can be seen in the polyploid hepatocyte nuclei (arrows), whereas single X and Y chromosome signals only are present in the myofibroblast nuclei (original magnification,  $\times 600$ ). (B–D) Confocal “image slices” through a single BM-derived myofibroblast nucleus demonstrating the presence of only single X and Y chromosomes.

chromosome, unlike mice that received BM enriched for male HSCs, in which only 8.2% (range, 7;  $n = 3$ ) of hepatic myofibroblasts contained the Y chromosome (Figure 9F). We therefore concluded that the predominant source of hepatic myofibroblasts within the BM is the MSCs. To determine whether the double lineage depletion population contained cells with a MSC phenotype, a proportion of these cells ( $1 \times 10^5$  cells/well in 6-well plates) were plated into Mesencult medium as before. This resulted in only occasional single plastic adherent cells after 1 week culture, and we failed to grow MSC colonies from these cells (Figure 9B). In contrast, 1 week after plating whole BM cells in Mesencult medium, cells frequently showed a typical MSC phenotype (Figure 9C).

## Discussion

Cirrhosis develops in the chronically damaged liver and is thought to occur by activation of stellate cells

into activated myofibroblasts, resulting in cell proliferation,  $\alpha$ -SMA expression, and collagen deposition.<sup>17,34</sup> However, hepatic myofibroblasts can display phenotypic heterogeneity,<sup>35,36</sup>  $\alpha$ -SMA-negative cells can produce intrahepatic collagen,<sup>37</sup> and BM-derived hepatic myofibroblasts have been identified.<sup>22</sup>

We have sought to study systematically the contribution of BM to hepatic stellate cells and myofibroblast cell populations. We first confirmed that the irradiation protocol used to deplete the recipients' BM did not deplete intrahepatic stellate cell numbers, and, therefore, we concluded that the findings in the transplantation mice mirror those occurring in nontransplantation mice. In the absence of liver damage, the proportion of BM-derived stellate cells remained at approximately 14% in the absence of liver damage. During the development of cirrhosis, we found an increase in the proportion of stellate cells of BM origin and total numbers of BM-derived myofibroblasts, suggesting an axis of recruitment from the BM, which is activated during tissue injury. Remarkably, by the time cirrhosis had developed, the majority of the hepatic myofibroblasts were of BM origin, indicating the importance of this axis in chronic hepatocellular liver damage. Following the recovery from liver injury, the proportion of stellate cells of BM origin fell markedly, suggesting an intrahepatic source of renewal. BM therapy has been suggested for the failing liver to replace hepatocyte mass. However, we could identify only a minor population of BM-derived hepatocytes. Our results contrast with findings using BM injections from a green fluorescent protein transgenic donor in a mouse model of cirrhosis, in which it was reported that much of the liver parenchyma could be repopulated by BM-derived cells.<sup>9</sup> Furthermore, it has been suggested that BM injections may abrogate the development of cirrhosis in the mouse CCl<sub>4</sub> model and, in contrast to our studies, few stellate cells of BM origin were identified.<sup>38</sup> One possible explanation for these seemingly contradictory results may be that our studies looked at the situation of BM transplantation mice with the aim of observing what is occurring typically in the pathogenesis of liver damage, whereas the studies by Terai et al<sup>9</sup> and Sakaida et al<sup>38</sup> look at BM injected into nonirradiated recipient mice. In these studies, it is unlikely that the donor BM engrafts the recipient BM and therefore is not subject to the influence of the BM stem cell niche, which may determine BM stem cell behavior.

We sought evidence of the *in vivo* functionality of BM-derived myofibroblasts and identified BM-derived myofibroblasts in the region of hepatic scarring that were transcriptionally active for collagen using 2 independent techniques: first, by the use of donor mice that had a

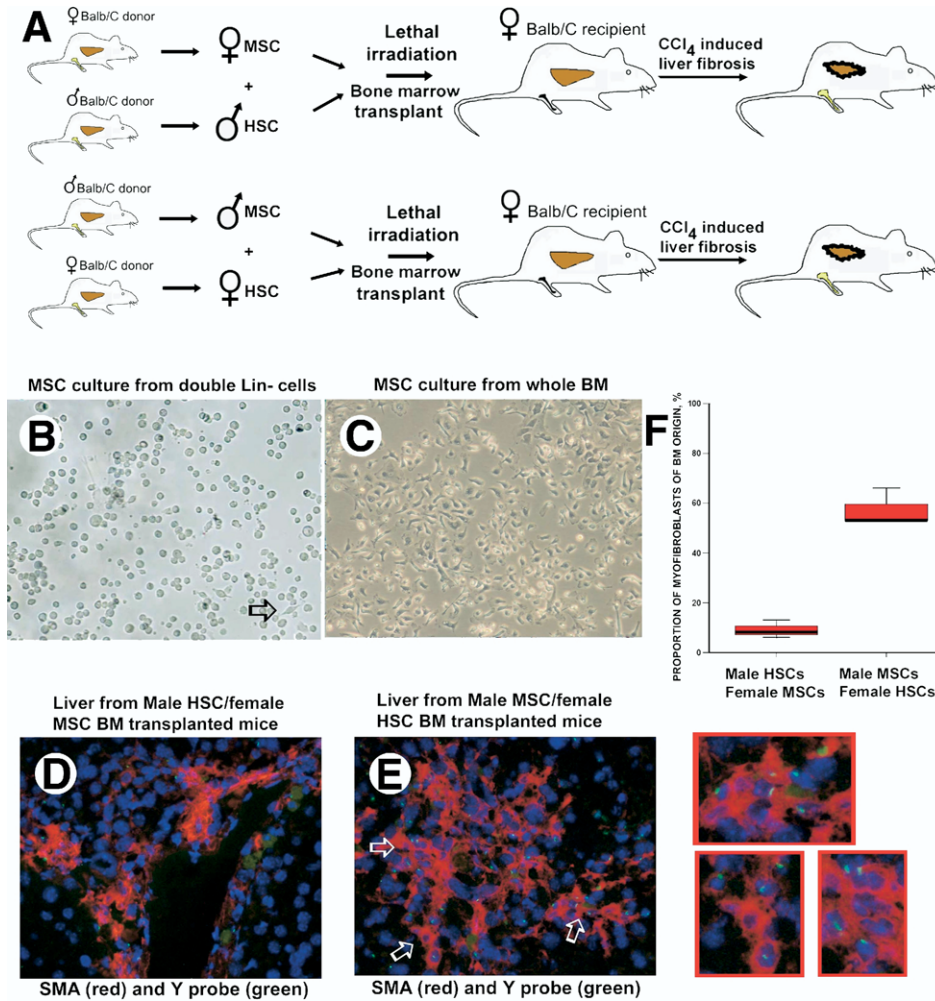


**Figure 9.** Analysis of the BM stem cell origin of hepatic myofibroblasts. (A) Six-week-old female Balb/c mice (n = 6) received lethal irradiation followed by transplants of BM, which was enriched for either female MSCs and male HSCs or female HSCs and male MSCs. Four weeks later, the mice received CCl<sub>4</sub> injections for 8 weeks. FISH for the Y chromosome in the livers was performed to track whether the BM-derived myofibroblasts were predominantly of MSC or HSC origin. MSC cells were enriched from whole BM by culture in Mesencult for 1 week, and the plastic-adherent cell population was used. To enrich for HSCs, double lineage depletion was performed. (B) To determine whether the double lineage depletion population contained cells with a MSC phenotype, a proportion of these cells (1 × 10<sup>5</sup> cells/well in 6-well plates) were plated into Mesencult medium as before. This resulted in only occasional single plastic adherent cells after 1-week culture, and we failed to grow MSC colonies from these cells. (C) In contrast, 1 week after plating whole BM cells in Mesencult medium, frequently, cells showed a typical MSC phenotype. (D) In mice that received male HSC and female MSC, the myofibroblasts (α-SMA, red) were largely Y chromosome (green) negative (original magnification, ×400). (E) In mice that received male MSC and female HSC, the myofibroblasts (α-SMA, red) were frequently Y chromosome (green) positive (original magnification, ×400). (F) The proportion of BM-derived hepatic myofibroblasts in mice that had received BM transplants with either male HSC/female MSC or male MSC/female HSC, suggesting that the predominant source of hepatic myofibroblasts within the BM are the MSCs. Figure shows median values (line), interquartile range (boxes), and range (whiskers). Enlarged examples from Figure 9E in red boxes.

marker gene that is activated in the presence of collagen transcription and, second, by performing dual ISH on liver sections with radioactive probes to detect the presence of collagen mRNA and fluorescent probes to detect Y chromosome DNA. Both techniques clearly indicated that the BM-derived cells transcribed collagen in the damaged liver. We therefore asked whether the phenotype of the BM-derived myofibroblasts influences the damaged organ's fibrotic response. Mice that received BM from the Col 1a1<sup>fl</sup> mice developed extensive and

characteristic pericellular fibrosis typical of the Col 1a1<sup>fl</sup> mouse, unlike control mice that had more restricted linear collagen deposition. This suggests that, by manipulating the phenotype of the BM-derived myofibroblasts, we can influence the injured organ's fibrotic response, and, as such, it may be possible to abrogate the damaged organ's fibrotic response by manipulation of this axis. We determined that the hepatic myofibroblasts of BM origin were predominantly from cells enriched for mesenchymal progenitor cells, although it is worth noting

there were also some BM-derived myofibroblasts that originated from cells enriched for HSCs. This may simply reflect an inability to purify cells absolutely, but it may also reflect a contribution to the BM-derived myofibroblast population from circulating fibrocytes of HSC origin.

In conclusion, in chronic liver injury, the BM has a minor role in hepatocyte regeneration but is a major source of functional hepatic stellate cells and myofibroblasts. This axis of organ fibrosis is worthy of further study and is a potential therapeutic target. The BM has therapeutic potential in organ damage, but it would seem prudent that such stem cells be tested in various models of organ damage to identify stem cell progeny in target and nontarget organs.

## References

- Jang YY, Collector MI, Baylin SB, Diehl AM, Sharkis SJ. Hematopoietic stem cells convert into liver cells within days without fusion. *Nat Cell Biol* 2004;6:532–539.
- Harris RG, Herzog EL, Bruscia EM, Grove JE, Van Arnem JS, Krause DS. Lack of a fusion requirement for development of bone marrow-derived epithelia. *Science* 2004;305:90–93.
- Ianus A, Holz GG, Theise ND, Hussain MA. In vivo derivation of glucose-competent pancreatic endocrine cells from bone marrow without evidence of cell fusion. *J Clin Invest* 2003;111:843–850.
- Kajstura J, Rota M, Whang B, Cascapera S, Hosoda T, Bearzi C, Nurzynska D, Kasahara H, Zias E, Bonafe M, Nadal-Ginard B, Torella D, Nascimbene A, Quaini F, Urbanek K, Leri A, Anversa P. Bone marrow cells differentiate in cardiac cell lineages after infarction independently of cell fusion. *Circ Res* 2005;96:127–137.
- Camargo FD, Finegold M, Goodell MA. Hematopoietic myelomonocytic cells are the major source of hepatocyte fusion partners. *J Clin Invest* 2004;113:1266–1270.
- Wagers AJ, Sherwood RI, Christensen JL, Weissman IL. Little evidence for developmental plasticity of adult hematopoietic stem cells. *Science* 2002;297:2256–2259.
- Overturf K, Al-Dhalimy M, Ou CN, Finegold M, Grompe M. Serial transplantation reveals the stem-cell-like regenerative potential of adult mouse hepatocytes. *Am J Pathol* 1997;151:1273–1280.
- Lagasse E, Connors H, Al-Dhalimy M, Reitsma M, Dohse M, Osborne L, Wang X, Finegold M, Weissman IL, Grompe M. Purified hematopoietic stem cells can differentiate into hepatocytes in vivo. *Nat Med* 2000;6:1229–1234.
- Terai S, Sakaida I, Yamamoto N, Omori K, Watanabe T, Ohata S, Katada T, Miyamoto K, Shinoda K, Nishina H, Okita K. An in vivo model for monitoring trans-differentiation of bone marrow cells into functional hepatocytes. *J Biochem (Tokyo)* 2003;134:551–558.
- Alison MR, Vig P, Russo F, Bigger BW, Amofah E, Themis M, Forbes S. Hepatic stem cells: from inside and outside the liver? *Cell Prolif* 2004;37:1–21.
- Kanazawa Y, Verma IM. Little evidence of bone marrow-derived hepatocytes in the replacement of injured liver. *Proc Natl Acad Sci U S A* 2003;100(Suppl 1):11850–11853.
- McTaggart RA, Feng S. An uncomfortable silence while we all search for a better reporter gene in adult stem cell biology. *Hepatology* 2004;39:1143–1146.
- Gao Z, McAlister VC, Williams GM. Repopulation of liver endothelium by bone-marrow-derived cells. *Lancet* 2001;357:932–933.
- Duffield JS, Forbes SJ, Constandinou CM, Clay S, Partolina M, Vuthoori S, Wu S, Lang R, Iredale JP. Selective depletion of macrophages reveals distinct, opposing roles during liver injury and repair. *J Clin Invest* 2005;115:56–65.
- Pinzani M, Rombouts K, Colagrande S. Fibrosis in chronic liver diseases: diagnosis and management. *J Hepatol* 2005;42:S22–S36.
- Friedman SL. Liver fibrosis—from bench to bedside. *J Hepatol* 2003;38(Suppl 1):S38–S53.
- Brenner DA, Waterboer T, Choi SK, Lindquist JN, Stefanovic B, Burchardt E, Yamauchi M, Gillan A, Rippe RA. New aspects of hepatic fibrosis. *J Hepatol* 2000;32:32–38.
- Brittan M, Hunt T, Jeffery R, Poulson R, Forbes SJ, Hodivala-Dilke K, Goldman J, Alison MR, Wright NA. Bone marrow derivation of pericyptal myofibroblasts in the mouse and human small intestine and colon. *Gut* 2002;50:752–757.
- Direkze NC, Forbes SJ, Brittan M, Hunt T, Jeffery R, Preston SL, Poulson R, Hodivala-Dilke K, Alison MR, Wright NA. Multiple organ engraftment by bone-marrow-derived myofibroblasts and fibroblasts in bone-marrow-transplanted mice. *Stem Cells* 2003;21:514–520.
- Hashimoto N, Jin H, Liu T, Chensue SW, Phan SH. Bone marrow-derived progenitor cells in pulmonary fibrosis. *J Clin Invest* 2004;113:243–252.
- Baba S, Fujii H, Hirose T, Yasuchika K, Azuma H, Hoppo T, Naito M, Machimoto T, Ikai I. Commitment of bone marrow cells to hepatic stellate cells in mouse. *J Hepatol* 2004;40:255–260.
- Forbes SJ, Russo FP, Rey V, Burra P, Ruge M, Wright NA, Alison MR. A significant proportion of myofibroblasts are of bone marrow origin in human liver fibrosis. *Gastroenterology* 2004;126:955–963.
- Yamamoto N, Terai S, Ohata S, Watanabe T, Omori K, Shinoda K, Miyamoto K, Katada T, Sakaida I, Nishina H, Okita K. A subpopulation of bone marrow cells depleted by a novel antibody, anti-Liv8, is useful for cell therapy to repair damaged liver. *Biochem Biophys Res Commun* 2004;313:1110–1118.
- am Esch JS, Knoefel WT, Klein M, Ghodsizad A, Fuerst G, Poll LW, Piechaczek C, Burchardt ER, Feifel N, Stoldt V, Stockschrader M, Stoecklein N, Tustas RY, Eisenberger CF, Peiper M, Haussinger D, Hosch SB. Portal application of autologous CD133+ bone marrow cells to the liver: a novel concept to support hepatic regeneration. *Stem Cells* 2005;23:463–470.
- Murphy FR, Issa R, Zhou X, Ratnarajah S, Nagase H, Arthur MJ, Benyon C, Iredale JP. Inhibition of apoptosis of activated hepatic stellate cells by tissue inhibitor of metalloproteinase-1 is mediated via effects on matrix metalloproteinase inhibition: implications for reversibility of liver fibrosis. *J Biol Chem* 2002;277:11069–11076.
- Bou-Gharios G, Garrett LA, Rossert J, Niederreither K, Eberspaecher H, Smith C, Black C, Crombrugge B. A potent far-upstream enhancer in the mouse pro  $\alpha$  2(I) collagen gene regulates expression of reporter genes in transgenic mice. *J Cell Biol* 1996;134:1333–1344.
- Inagaki Y, Truter S, Bou-Gharios G, Garrett LA, de Crombrugge B, Nemoto T, Greenwel P. Activation of Pro $\alpha$ 2(I) collagen promoter during hepatic fibrogenesis in transgenic mice. *Biochem Biophys Res Commun* 1998;250:606–611.
- Issa R, Zhou X, Trim N, Millward-Sadler H, Krane S, Benyon C, Iredale J. Mutation in collagen-1 that confers resistance to the action of collagenase results in failure of recovery from CCl<sub>4</sub>-induced liver fibrosis, persistence of activated hepatic stellate cells, and diminished hepatocyte regeneration. *FASEB J* 2003;17:47–49.
- Olmsted-Davis EA, Gugala Z, Camargo F, Gannon FH, Jackson K, Kienstra KA, Shine HD, Lindsey RW, Hirschi KK, Goodell MA, Brenner MK, Davis AR. Primitive adult hematopoietic stem cells

- can function as osteoblast precursors. *Proc Natl Acad Sci U S A* 2003;100:15877–15882.
30. Han W, Ye Q, Moore MA. A soluble form of human  $\Delta$ -like-1 inhibits differentiation of hematopoietic progenitor cells. *Blood* 2000;95:1616–1625.
  31. Peters BA, Diaz LA, Polyak K, Meszler L, Romans K, Guinan EC, Antin JH, Myerson D, Hamilton SR, Vogelstein B, Kinzler KW, Lengauer C. Contribution of bone marrow-derived endothelial cells to human tumor vasculature. *Nat Med* 2005;11:261–262.
  32. Willenbring H, Bailey AS, Foster M, Akkari Y, Dorrell C, Olson S, Finegold M, Fleming WH, Grompe M. Myelomonocytic cells are sufficient for therapeutic cell fusion in liver. *Nat Med* 2004;10:744–748.
  33. Wang X, Willenbring H, Akkari Y, Torimaru Y, Foster M, Al-Dhalimy M, Lagasse E, Finegold M, Olson S, Grompe M. Cell fusion is the principal source of bone-marrow-derived hepatocytes. *Nature* 2003;422:897–901.
  34. Arthur MJ, Mann DA, Iredale JP. Tissue inhibitors of metalloproteinases, hepatic stellate cells and liver fibrosis. *J Gastroenterol Hepatol* 1998;13(Suppl):S33–S38.
  35. Ramadori G, Saile B. Mesenchymal cells in the liver—one cell type or two? *Liver* 2002;22:283–294.
  36. Cassiman D, Libbrecht L, Desmet V, Deneff C, Roskams T. Hepatic stellate cell/myofibroblast subpopulations in fibrotic human and rat livers. *J Hepatol* 2002;36:200–209.
  37. Magness ST, Bataller R, Yang L, Brenner DA. A dual reporter gene transgenic mouse demonstrates heterogeneity in hepatic fibrogenic cell populations. *Hepatology* 2004;40:1151–1159.
  38. Sakaida I, Terai S, Yamamoto N, Aoyama K, Ishikawa T, Nishina H, Okita K. Transplantation of bone marrow cells reduces CCl<sub>4</sub>-induced liver fibrosis in mice. *Hepatology* 2004;40:1304–1311.
- 
- Received April 20, 2005. Accepted January 4, 2006.
- Address requests for reprints to: Stuart J. Forbes, MD, Tissue Fibrosis and Repair Group, MRC University of Edinburgh Centre for Inflammation Research, The Queen's Medical Research Institute, 47 Little France Crescent, Edinburgh EH16 4TJ, UK. e-mail: s.j.forbes@imperial.ac.uk; fax: (44) 207 886 1931.
- Supported by an Advanced Fellowship from The Wellcome Trust (to S.J.F.) and a Sheila Sherlock Fellowship from the European Association for the Study of the Liver (to F.P.R.).
- The authors thank Professor Steven Krane (Center for Immunology and Inflammatory Diseases, Department of Medicine, Harvard Medical School and Massachusetts General Hospital) for supplying the Col1a1<sup>fl</sup> mice.